Clay Minerals, (2015) **50**, 91–101

Uptake of Pb and Zn from a binary solution onto different fixed bed depths of natural zeolite – the BDST model approach

I. NUIĆ*, M. TRGO, J. PERIĆ AND N. VUKOJEVIĆ MEDVIDOVIĆ

Faculty of Chemistry and Technology, University of Split, Teslina 10/V, 21000 Split, Croatia

(*Received 14 July 2014; revised 21 January 2015; Guest Editor A. Langella*)

ABSTRACT: The removal of lead and zinc from a binary solution by fixed bed depths (40, 80 and 120 mm) of a natural zeolite was examined at a flow rate of 1 mL/min. The results obtained were fitted to the Bed Depth Service Time (BDST) model and the parameters of the model (q and k) were used to design a column system for flow rates of 2 and 3 mL/min at a bed depth of 80 mm. The experimental results were in excellent agreement with those predicted and experimental breakthrough curves for the binary systems were obtained. This approach facilitates the design of effective binary column processes without additional experimentation. Two major design parameters, the Empty Bed Contact Time (*EBCT*) and the zeolite usage rate, were calculated. The highest *EBCT* value of 13.56 min represents the optimal conditions for the binary (Pb+Zn) solution.

KEYWORDS: lead, zinc, binary solution, natural zeolite, fixed bed, BDST model.

Continuous population growth and the development of industrial processes are the major contributors to increasing concentrations of heavy metals in the biosphere. Industrial wastewaters are considered to be the greatest source of pollution by heavy metals. The environment is contaminated with lead from anthropogenic sources as well as from natural geochemical processes. Lead is used widely as the raw material in many important industrial applications, such as the manufacture of storage batteries, pigments, fuels, explosives, photographic materials and coatings for the automotive, aeronautical and steel industries. Lead is a non-essential element, extremely toxic to living organisms and, if released into the environment, can bio-accumulate through the food chain. It damages the nervous system, causes mental retardation, interferes with normal cellular metabolism and reduces production of the haemoglobin necessary for oxygen transport. In addition, lead can damage the kidneys and reproductive system, particularly in children (Alloway & Ayres, 1993; Qaiser *et al*., 2007; Bueno *et al*., 2008). Zinc is present in wastewaters from metallurgical processes, galvanizing plants, stabilizers, thermoplastics, pigments, alloys and battery manufacture. In addition, there are usually elevated levels of zinc in the discharges from municipal wastewater treatment plants. Zinc is an essential trace element and plays a role in electron transfer in many enzymatic reactions in humans. However, its prolonged and excessive intake may lead to toxic effects such as carcinogenesis, mutagenesis and teratogenesis as a result of bioaccumulation (El-Shafey, 2010).

The removal of heavy metals from wastewaters to give concentrations below the permissible limits requires the application of advanced wastewater treatment processes such as adsorption, ion exchange and membrane techniques. The excellent

* E-mail: ivona@ktf-split.hr
DOI: 10.1180/claymin.2015.050.1.09

physical and chemical properties of natural zeolites, their high adsorption capacity, the wide distribution of deposits and their low cost of exploitation, contribute to their application in wastewater treatment. The efficient performance of ion exchange columns using natural zeolites makes it possible to treat large quantities of wastewater. Furthermore, the ease of regeneration of the zeolite through several service/regeneration cycles makes zeolite-based ion exchange even more attractive. The removal of heavy-metal ions from multi-component solutions onto natural zeolite is a complex problem because of the competition between the ions, a consequence of their different affinities as well as the selectivity of the zeolite.

The application of the column process requires a basic knowledge of the mass-transfer mechanism between the liquid and solid phase. Specifically, fixed bed operations are affected by equilibrium (isotherm, capacity), kinetic (diffusion and convection coefficients) and hydraulic (liquid holdup, geometric analogies and mal-distribution) factors (Inglezakis, 2010). As the breakthrough curves best describe the effective binding of Pb and Zn ions within a fixed zeolite bed, it is of great importance to be able to predict them reliably and hence, calculate the breakthrough and exhaustion points for various experimental conditions. For this purpose, various mathematical kinetic models have been developed to facilitate the design and analysis of sorption systems (Inglezakis *et al*., 2003; Hamdaoui, 2009; Trgo *et al*., 2011). In a previous study (Nuić *et al*., 2013), the Thomas model, which is an empirical equation that ignores the intra-particle (solid) mass-transfer resistance and the external liquid-film resistance (Inglezakis, 2010), was applied to the binary (Pb+Zn) solutions. The model gave very good agreement with the experimental data up to the exhaustion point, after which slight deviations occurred. Comparison of the application of the Thomas model to single ion and binary ion solutions under the same experimental conditions (Trgo *et al*., 2011), showed a better fit with the experimental data for the single-ion solutions.

Among the different mathematical models found in the literature, the Bed Depth Service Time (BDST) model offers a simple and rapid method of designing the fixed bed column. It correlates the service time, at which the effluent concentration would not exceed the defined value, with a certain bed depth for a given set of conditions (McKay *et al*., 1998; Cooney, 1999; Ko *et al*., 2000; Lodeiro *et al*., 2006; Vijayaraghavan & Praba, 2006; Hun *et al*., 2007; Wan Ngah *et al*., 2012; Rajeshkannan *et al*., 2013). The BDST model has rarely been applied to a fixed bed of natural zeolite or to binary metal solutions.

This study describes lead and zinc uptake from an equimolar binary solution on different zeolite fixed bed depths using the BDST model approach. The calculated parameters of the BDST model can be used for calculation of the operating data under various experimental conditions, including the flow rate, which is important for the design of fixed bed columns without additional experimentation.

MATERIALS AND METHODS

Preparation of the zeolite sample

The raw zeolite sample used in these experiments originates from the Zlatokop deposit in Vranjska Banja (Serbia). The zeolite was milled and sieved to the particle size of 0.6−0.8 mm, rinsed with ultrapure water to remove impurities, dried at 60ºC and stored in a desiccator. The chemical composition of the zeolite sample was determined by classical chemical analysis, as follows (in mass%): SiO_2, 66.36; Al_2O_3, 13.81; Fe_2O_3, 1.69; MgO, 1.03; CaO, 3.65; K_2O, 0.99; Na_2O, 1.03 and loss on ignition (LOI) 13.40. Semi-quantitative mineralogical analysis has shown that the zeolite sample contained up to 80% of clinoptilolite as the major mineralogical component, with quartz as an impurity (Vukojević Medvidović *et al*., 2006). The theoretical exchange capacity of the zeolite sample has been calculated from the chemical composition as 1.411 mmol/g (Nuić *et al*., 2013). The main exchangeable cation of the zeolite was calcium.

Preparation of the binary heavy metal solution

The equimolar binary solution of lead and zinc ions was prepared by dissolving $Pb(NO_3)_2$ and $Zn(NO_3)_2{\cdot}6H_2O$ in ultrapure water, without pH adjustment (the initial pH value was ~4.5). Under these experimental conditions, the precipitation of metal hydroxides does not occur. The total concentration of the binary solution was constant and equalled $c_o \approx 1$ mmol/L, with the lead and zinc concentration ratio of $c_o(Pb)/c_o(Zn) \approx 1$. The regeneration solution was prepared by dissolving $NaNO_3$, c = 176.5 mmol/L, in ultrapure water.

https://doi.org/10.1180/claymin.2015.050.1.09 Published online by Cambridge University Press

Column experiments

Laboratory column tests were carried out isothermally at ambient temperature in 500 mm-long glass columns, with 12 mm internal diameter, with zeolite sample-bed-depths of 40, 80 and 120 mm. These depths correspond to bed volumes of 4.52, 9.04 and 13.56 cm^3, or 2.9, 5.9 and 8.9 g of zeolite, respectively. The binary solution of lead and zinc cations was passed down through the beds at a constant flow rate of Q = 1 mL/min, with the aid of a vacuum pump. After each service cycle, the exhausted zeolite bed was regenerated with $NaNO_3$ solution (176.5 mmol/L) at a flow rate of 1 mL/min, under the same operating conditions. In all experiments, the effluent samples were collected periodically and analysed for Zn concentration using a Methrom 761 Compact IC liquid chromatograph and for the total (Pb+Zn) concentration by the complexometric method. For the application of the BDST model, experiments were performed at the bed depth of 80 mm under the same operating conditions, but at flow rates of 2 and 3 mL/min.

SEM/EDS analysis

Scanning electron microscopy (SEM) and energy-dispersive spectrometry (EDS) analysis (Jeol Scanning Microscope - 6610LV) was performed with zeolite samples taken from the top of the 80 and 120 mm zeolite beds after each service cycle and before regeneration. For the bed depth of 80 mm, the analysis was performed with a magnification of 100× and the mapping analysis was done at selected surfaces on the image. Secondary electron (SE) images and back-scattered electron (BSE) images were obtained. For a bed depth of 120 mm, SEM/EDS semi-quantitative elemental analyses were performed with a magnification of 100×. Zeolite samples of both bed depths examined were milled to powder and analysed by SEM/EDS in order to observe the distribution of elements through the particles.

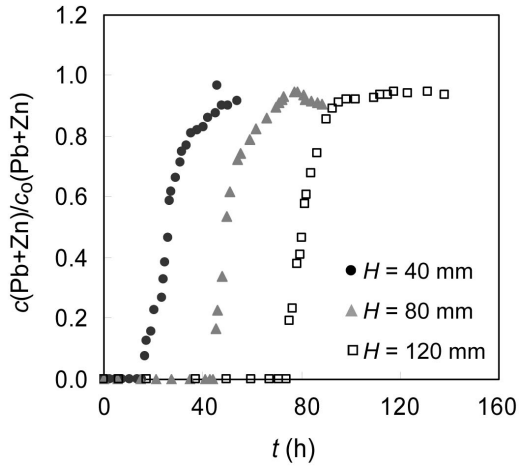

FIG. 1. Breakthrough curves at bed depths of 40, 80 and 120 mm at a flow rate of 1 mL/min.

RESULTS AND DISCUSSION

The effect of zeolite bed depth on Pb and Zn removal

Breakthrough curves obtained at three different zeolite bed depths and at a constant flow rate of 1 mL/min are shown in Fig. 1, as the ratio of the total (Pb+Zn) effluent and influent concentration *vs*. service time. The characteristic parameters of the breakthrough curves were calculated according to Nuić *et al*. (2013) and are listed in Table 1.

All breakthrough curves follow the characteristic S-shaped profile. As expected, with increasing bed

TABLE 1. Experimental and calculated parameters of the breakthrough curves at bed depths of 40, 80 and 120 mm at a flow rate of 1 mL/min.

H (mm)	t_B (h)	V_B (L)	t_E (h)	V_E (L)	h_Z (mm)	q_B (mmol (Pb+Zn)/g)	q_E (mmol (Pb+Zn)/g)	n_R (mmol (Pb+Zn))
40	16.66	1.00	46.33	2.78	38.90	0.336	0.594	1.423
80	45.25	2.72	73.08	4.39	42.95	0.430	0.511	4.066
120	75.08	4.51	101.83	6.11	38.77	0.508	0.562	5.408

https://doi.org/10.1180/claymin.2015.050.1.09 Published online by Cambridge University Press

depth, the time necessary for breakthrough (t_B) and exhaustion (t_E) increases and a greater volume of solution is treated (V_B, V_E). With increasing bed depth the time between the breakthrough and exhaustion points decreases (Lodeiro *et al*., 2006; Hun *et al*., 2007). The breakthrough capacity q_B increases with increasing bed depth, while the exhaustion capacity q_E does not change. The height h_Z of the mass transfer zone (MTZ) was calculated according to Nuić *et al*. (2013) and is presented in Table 1.

Regeneration curves, obtained after each service cycle, are shown in Fig. 2 as the total (Pb+Zn) concentration in the regeneration eluent *vs*. time.

The quantities of Pb and Zn cations eluted during the regeneration cycles increases with bed depth (Fig. 2) as confirmed by the quantities, n_R, of eluted (Pb+Zn) ions listed in Table 1. The volume of eluent necessary for completion of the regeneration cycle was between 0.37 L and 0.84 L, i.e. 18−13% of the volume of the solution treated in the service cycle.

Analysis of the SEM/EDS results

Analysis by SEM/EDS is useful for studying metal sorption on sorbent surfaces, as well as for the visualization of metal–sorbent interactions (Remenárová *et al*., 2012). Figure 3a shows a BSE image of the zeolite particle surface taken from the bed of depth 80 mm. The uniform colour of the solid phase indicates uniformity in chemical and mineralogical composition, suggesting that precipitates were not formed during the heavy-metal uptake from the binary solution. In the SE image, the EDS analyses of each surface are very similar, confirming the uniform chemical composition (Fig. 3b,c). Among all analysed elements, the content of Pb is dominant (20.69% Pb) compared to Zn (0.46% Zn). The Na-content is higher compared to the content of other exchangeable cations due to the regeneration of zeolite with sodium nitrate solution.

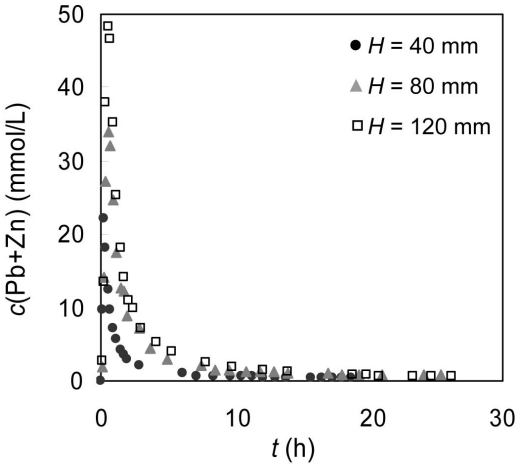

FIG. 2. Regeneration curves for (Pb+Zn) at bed depths of 40, 80 and 120 mm.

Figure 4 shows a SE image of a particle sample taken from the top of the bed of depth 120 mm, with three EDS spectra. The EDS analysis also shows a uniform composition; Pb again dominates over Zn (20.51% Pb and 0.38% Zn). The higher concentration of Pb compared to Zn indicates the probable displacement of bound zinc ions by lead.

Both zeolite samples were milled to powder and analysed again by EDS. The results showed the same elemental composition as on the particle surface, confirming that the ion binding process takes place throughout the volume of the particle.

Application of the BDST kinetic model

The original equation of the Bed Depth Service Time (BDST) approach simplified model was proposed by Bohart & Adams for the design of carbon adsorption columns (Benefield *et al*., 1982). Their equation is based on the surface reaction rate theory and can be expressed as follows:

$$\ln\left(\frac{c_o}{c}-1\right)=\ln\left(e^{\left(kq\frac{H}{v}\right)}-1\right)-kc_o t \qquad (1)$$

where: c_o is the influent solute concentration (mmol/L), c is the effluent solute concentration (mmol/L), k is the rate constant for the transfer of solute from the fluid phase to the solid phase (L/mmol h), q is the removal capacity of the zeolite (mmol/L), H is the depth of the zeolite bed (m), v is the linear velocity of the influent (m/h) and t is the service time (h).

For $e^{kq\frac{H}{v}} >> 1$ in equation 1, a linear relationship between the bed depth and service time was obtained:

$$t=\frac{q}{c_o v}H-\frac{1}{kc_o}\ln\left(\frac{c_o}{c}-1\right) \qquad (2)$$

This form of the equation makes it possible to calculate the model parameters q and k from the

https://doi.org/10.1180/claymin.2015.050.1.09 Published online by Cambridge University Press

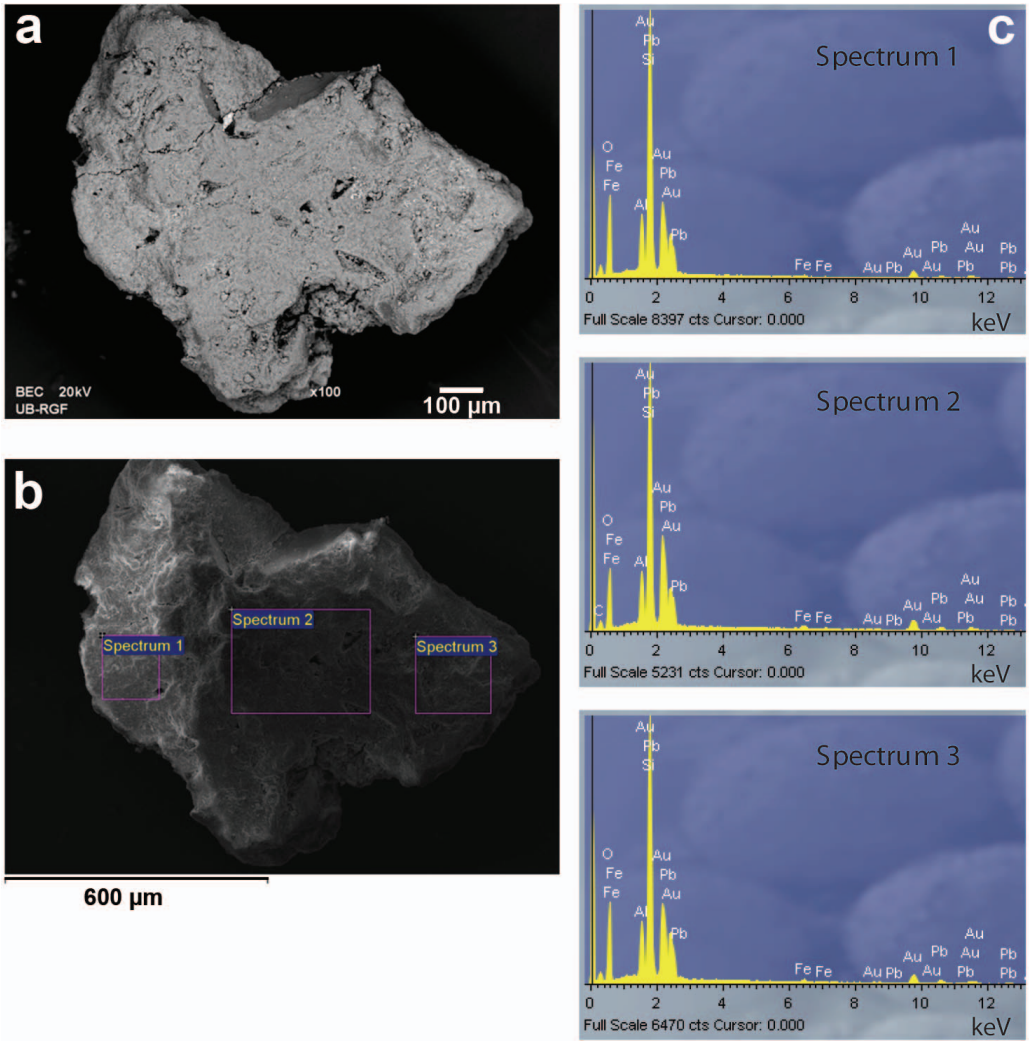

FIG. 3. SEM images of a crystal particle taken from the top surface of the exhausted zeolite from the 80 mm depth bed: (a) BSE image × 100, (b) SE image × 100 with three areas selected for EDS analysis, (c) EDS analysis of the three areas. Note: Mean wt.% of Pb, Zn and exchangeable cations from the three selected spectra: 20.69% Pb, 0.46% Zn, 0.17% Na, 0.21% K, 0.00% Ca and 0.07% Mg.

experimental data for service time t at a certain bed depth H. Setting $t = 0$ gives the intercept of the abscissa, which represents the theoretical critical bed depth, H_o:

$$H_o = -\frac{v}{kq}\ln\left(\frac{c_o}{c} - 1\right) \qquad (3)$$

where: H_o is the minimum depth for obtaining satisfactory effluent concentration at $t = 0$.

At least nine individual column tests must be performed to collect the laboratory data required for the Bohart-Adams approach, which is very expensive and time consuming. Therefore, a modification of the Bohart-Adams model was proposed, which requires only three column tests to collect the necessary data (Benefield *et al.*, 1982; Vijayaraghavan & Praba, 2006; Perić *et al.*, 2009; Trgo *et al.*, 2011). In this method, known as the Bed Depth Service Time (BDST) approach, the Bohart-Adams equation is expressed as:

$$t = aH + b \qquad (4)$$

https://doi.org/10.1180/claymin.2015.050.1.09 Published online by Cambridge University Press

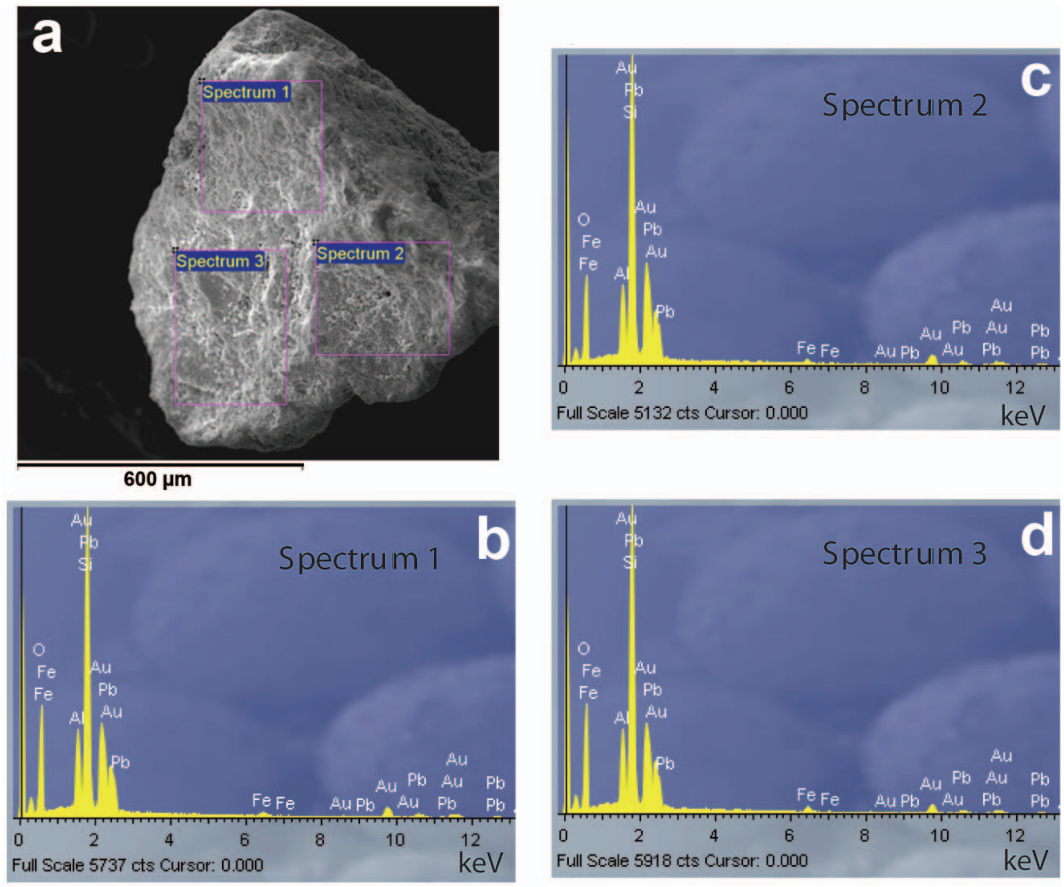

FIG. 4. (a) SE image of a crystal particle taken from the top surface of the exhausted zeolite from the 120 mm depth bed (100×) with three areas selected for analysis and (b–d) EDS analysis of the three selected areas. Note: Mean wt.% of Pb, Zn and exchangeable cations for the three selected spectra: 20.51% Pb, 0.38% Zn, 0.11% Na, 0.00% K, 0.07% Ca and 0.04% Mg.

This approach enables the use of the bed-depth service-time data determined from a set of breakthrough curves (e.g. Fig. 1), when a concentration c in the effluent is reached. In order to develop a BDST correlation, the experimental breakthrough time curves obtained at certain (Pb+Zn) removal percentages of 95, 70, 50, 40, 25 and 5% were plotted against each bed depth. The t–H lines obtained are shown in Fig. 5.

The slope a of the t–H line represents the time required for the mass transfer zone (MTZ) to move down a unit length through the zeolite bed under selected experimental conditions:

$$a = \frac{q}{c_o v} \tag{5}$$

The intercept b of the ordinate axis in Fig. 5 represents the time required for the adsorption zone to pass through the critical bed depth H_o:

$$b = -\frac{1}{kc_o}\ln\left(\frac{c_o}{c} - 1\right) \tag{6}$$

From the slope a and intercept b of the respective lines presented in Fig. 5, the parameters of the BDST model, q and k, were calculated assuming the influent concentration and linear velocity to be constant during the continuous operation. The parameters obtained are listed in Table 2.

The mass transfer zone (MTZ) is the zeolite layer through which the effluent concentration varies from 95% to 5% of the influent concentration. The

https://doi.org/10.1180/claymin.2015.050.1.09 Published online by Cambridge University Press

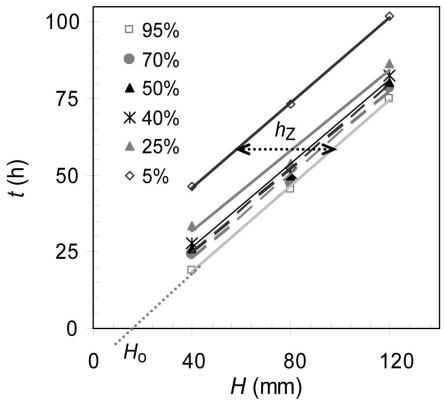

FIG. 5. The linear dependence of the service time at chosen removal percentages for the bed depths: 40, 80 and 120 mm ($c_o \approx 1$ mmol/l; $Q = 1$ mL/min).

mean height of the MTZ calculated for bed depths of 40, 80 and 120 mm and the flow rate of 1 mL/min is 40.21 mm (Table 1), which is approximately equal to the value, h_Z (39.57 mm), obtained by experiment (Fig. 5). The calculated value of H_o at breakthrough is 13.5 mm, suggesting a good selection of bed depths for this system.

The values of coefficient of determination obtained are high ($R^2 > 0.988$) indicating the validity of the BDST model for the present system. The value of the rate constant k varies from the breakthrough to the exhaustion point. If k is large, even a short bed will avoid breakthrough (Cooney, 1999). A lower value of k leads to an early breakthrough. The value of k decreases with the decrease in removal percentages (Table 2), but a significant change in its value is evident at 40–50% of removal, which corresponds to the inflection area of the breakthrough curves. This is probably related to the change in the mechanism of the process and correlates with data obtained using the Thomas model for the binary (Pb+Zn) system (Nuić *et al*., 2013), where the area between the inflection and exhaustion points on the breakthrough curves indicated a change in the mass transfer mechanism. With decreasing removal percentages (Table 2) there were no significant changes in the values of the removal capacities, which showed good agreement with the capacities obtained experimentally at the exhaustion point. Very similar capacity values were also obtained by applying the Thomas model (Nuić *et al*., 2013). Based on the calculated parameters, the BDST model has been used for estimation of the breakthrough curve under other working conditions.

TABLE 2. Experimental data at bed depths of 40, 80 and 120 mm and at flow rate of 1 mL/min and calculated BDST model parameters.

(Pb+Zn) removal (%)	Service time (h)			t -H line	R^2	k (L/mmol·h)	q (mmol/L)	q (mmol/g)	H_o (mm)
	H = 40 mm	H = 80 mm	H = 120 mm						
95	19.17	45.25	75.08	$t = 0.699 \cdot H - 9.41$	0.999	0.306	384.85	0.592	13.5
70	24.33	47.67	78.58	$t = 0.678 \cdot H - 4.06$	0.994	0.203	373.39	0.574	
50	26.00	49.75	80.42	$t = 0.680 \cdot H - 2.36$	0.995	0.013	374.55	0.576	
40	27.67	50.92	82.42	$t = 0.684 \cdot H - 1.08$	0.993	–*	376.86	0.580	
25	33.67	53.92	86.33	$t = 0.658 \cdot H + 5.31$	0.983	0.192	362.49	0.558	
5	46.33	73.08	101.83	$t = 0.694 \cdot H + 18.25$	0.999	0.150	382.04	0.588	

* The value k is not listed for 40% (Pb+Zn) removal due to its negative value.

https://doi.org/10.1180/claymin.2015.050.1.09 Published online by Cambridge University Press

TABLE 3. Comparison of the service time, at different breakthrough percentages, calculated from the BDST model and obtained experimentally at a bed depth of 80 mm and at flow rates of 2 and 3 mL/min.

(Pb+Zn) removal (%)	Q = 2 mL/min		Q = 3 mL/min	
	t_{mod} (h)	t_{exp} (h)	t_{mod} (h)	t_{exp} (h)
95	18.55	18.17	9.23	11.75
70	23.07	21.46	14.03	13.00
50	24.84	24.75	15.78	15.50
40	26.30	26.83	17.17	16.97
25	31.65	34.04	22.86	22.78
5	46.00	49.21	36.75	32.69

Design of the column process by the BDST model for different flow rates

According to the BDST approach, *t–H* lines (Table 2) determined at the flow rate of 1 mL/min and the influent concentration of 1 mmol/L, were used to predict the BDST equations for different flow rates. If the value of the original slope a is determined at a specific flow rate (at each of the three bed depths), the value of the new slope for desired flow rates can be calculated as follows (Benefield *et al*., 1982):

$$a_1 = a\left(\frac{v}{v_1}\right) \quad (7)$$

where: a and a_1 are the original and the new slope (h/mm) and v and v_1 are the original and the new linear velocity (mm/h). As $v = Q/A$, where A is the cross-sectional area of the column (cm^2), equation 7 can be written as follows:

$$a_1 = a\left(\frac{Q}{Q_1}\right) \quad (8)$$

where: Q and Q_1 are the original and the new flow rate (cm^3/min), respectively. The value of the rate constant k is determined by the net effect of mass transfer in the fluid, (which typically varies with linear velocity) and the mass transfer in the solid (which is independent of linear velocity). Since the solid-phase mass transfer resistance is usually dominant, k is not affected significantly by a change in linear velocity (Cooney, 1999). Thus, the intercept b (equation 6) in the BDST equation remains unchanged.

Inserting a values, from the *t–H* lines (Table 2) and Q and Q_1 values into equation 8, yielded new slopes a_1. When they were further integrated into equation 4 with the original intercepts b, BDST equations for the bed depth of 80 mm and new flow rates of 2 and 3 mL/min were calculated. In this way the predicted breakthrough time, t_{mod}, at certain removal percentages were obtained, which are listed in Table 3.

This method of estimating the service time under new conditions was only approximate. In order to evaluate the reliability of the results provided by the BDST model, new experiments were carried out at a bed depth of 80 mm and flow rates of 2 and 3 mL/min. Table 3 shows the comparison of the model and experimental values of breakthrough times (t_{mod} and t_{exp}) at defined removal percentages. The comparison of breakthrough curves predicted by the model (lines) and those confirmed by the experiments (symbols) is shown in Fig. 6.

A very good agreement of predicted and experimental results is observed. At the flow rate of 2 mL/min, complete overlapping of model and

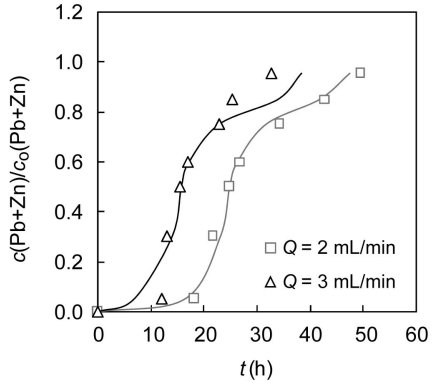

FIG. 6. Comparison of the predicted (lines) and experimental (symbols) breakthrough curves at a bed depth of 80 mm.

https://doi.org/10.1180/claymin.2015.050.1.09 Published online by Cambridge University Press

TABLE 4. Height of the mass transfer zone, empty bed contact times and zeolite usage rate calculated for different bed depths and flow rates.

H (mm)	m_Z (g)	Q (mL/min)	h_Z (cm)	$EBCT$ (min)	v_u (g/L)
40	2.9	1	38.90	4.52	2.52
80	5.9	1	42.95	9.04	2.17
120	8.9	1	38.77	13.56	1.98
80	5.9	2	47.63	4.52	2.71
80	5.9	3	50.31	3.01	2.79

experimental breakthrough curves was achieved. At the higher flow rate of 3 mL/min there were slight deviations particularly after the inflection area of the breakthrough curve. This may be due to the reduced contact time and therefore lower diffusivity of the Pb and Zn ions from the solution through the zeolite particles.

In order to optimize the liquid–solid contact time and removal capacity, it is necessary to find the relationship between the Empty Bed Contact Time (*EBCT*) and the zeolite usage rate (v_u) at the bed depths and flow rates examined. The *EBCT* is a critical parameter that represents the residence time during which the solution being treated is in contact with the zeolite, and includes bed depth and the linear flow rate as follows:

$$EBCT = \frac{H}{v} = \frac{H}{Q/A} = \frac{d^2\pi H}{4Q} \qquad (9)$$

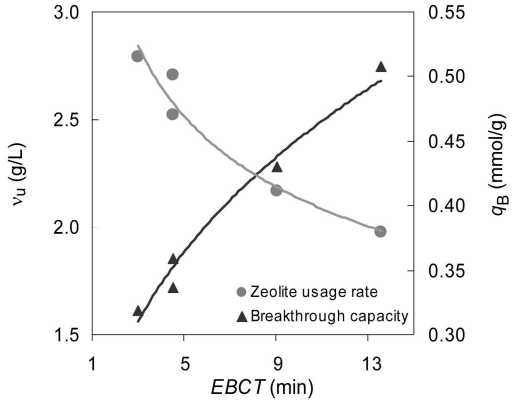

FIG. 7. Dependence of the zeolite usage rate and the removal capacity at breakthrough on the empty bed contact time.

The zeolite usage rate (Cooney, 1999; Ko *et al*., 2000; Gutiérrez-Segura *et al*., 2013) is a parameter of practical significance and equals:

$$v_u = \frac{m_Z 1000}{V_B} \qquad (10)$$

where: v_u is the zeolite usage rate (g/L), m_Z is the mass of zeolite in the bed (g), and V_B is the volume of the effluent treated at breakthrough (mL). The calculated *EBCT* and v_u values are presented in Table 4.

The zeolite usage rate and removal capacity at breakthrough were plotted *vs*. the EBCT values (Fig. 7), where at prolonged *EBCT* less zeolite is needed per unit volume of influent treated (Cooney, 1999).

The best *EBCT* is in the region where the zeolite usage rate is near its minimum value. The highest *EBCT* value of 13.56 min represents the optimal conditions for the binary (Pb+Zn) solution (Fig.7).

CONCLUSIONS

The Pb and Zn removal from binary aqueous solution by different fixed bed depths of natural zeolite has been tested. With an increase in bed depth, breakthrough and exhaustion times appear later and a greater volume of metal cation solution will be treated. The removal capacity at breakthrough increases with the bed depth while the capacity at exhaustion remains unchanged. The regeneration of the zeolite fixed bed was achieved successfully, which permitted the same zeolite to be reused multiple times without reducing its adsorption capacity. The zeolite particles had a uniform composition with lead, rather than zinc, being the dominant cation adsorbed, probably due to the displacement of bound zinc by the larger lead ions.

https://doi.org/10.1180/claymin.2015.050.1.09 Published online by Cambridge University Press

The ion adsorption took place throughout the volume of the zeolite particles. The BDST model approach gives an adequate description of the ion exchange of Pb and Zn from the binary solution into the zeolite bed using the column mode, under all experimental conditions studied. The calculated parameters q and k of the BDST model, at defined process conditions, were used successfully for the prediction of breakthrough time for new flow rates. The validity of the model and predicted results were confirmed experimentally. The BDST model could be used to optimize the design and performance of a fixed-bed scale-up with natural zeolite, for removal of Pb and Zn from binary aqueous solution. Its application is of great importance for practical use because it provides fast and easy assessment and description of experimental results, as well as enabling scaling up of the process for other conditions, e.g. different bed depths and flow rates, without additional experimentation. Two parameters of practical significance, *EBCT* and v_u, were calculated and compared. The optimal conditions for the binary (Pb+Zn) solution are at the highest *EBCT* value of 13.56 min.

ACKNOWLEDGMENT

This study was supported by the Croatian Science Foundation under the project HRZZ-NAZELLT IP-11-2013-4981.

REFERENCES

Alloway B.J. & Ayres D.C. (1993) Inorganic pollutants. Pp. 140–164 in: *Chemical Principles of Environmental Pollution, Part 2*. Blackie Academic & Professional. Chapman & Hall, Glasgow, UK.

Benefield L. D., Judkins J.F. & Weand B.L. (1982) Removal of soluble organic materials from wastewater by carbon adsorption. Pp. 365–404 in: *Process Chemistry for Water and Wastewater Treatment*. Prentice-Hall Inc., New Jersey, USA.

Bueno B.Y.M., Torem M.L., Molina F. & De Mesquita L.M.S. (2008) Biosorption of lead(II), chromium(III) and copper(II) by R. opacus: Equilibrium and kinetic studies. *Minerals Engineering*, **21**, 65–75.

Cooney D.O. (1999) Design of granular carbon fixed-bed adsorbers. Pp. 157–183 in: *Adsorption Design for Wastewater Treatment*. CRC Press, Boca Raton, Florida, USA.

El-Shafey E.I. (2010) Removal of Zn(II) and Hg(II) from aqueous solution on a carbonaceous sorbent chemically prepared from rice husk. *Journal of Hazardous Materials*, **175**, 319–327.

Gutiérrez-Segura E., Colín-Cruz A., Solache-Rios M. & Fall C. (2012) Removal of denim blue from aqueous solutions by inorganic adsorbents in a fixed-bed column. *Water, Air & Soil Pollution*, **223**, 5505–5513.

Hamdaoui O. (2009) Removal of copper(II) from aqueous phase by Purolite C100-MB cation exchange resin in fixed bed columns: Modelling. *Journal of Hazardous Materials*, **161**, 737–746.

Han R., Wang Y., Yu W., Zou W., Shi J. & Liu H. (2007) Biosorption of methylene blue from aqueous solution by rice husk in a fixed-bed column. *Journal of Hazardous Materials*, **141**, 713–718.

Inglezakis V.J. & Grigoropoulou H.P. (2003) Modelling of ion exchange of Pb^{2+} in fixed-beds of clinoptilolite. *Microporous and Mesoporous Materials*, **61**, 273–282.

Inglezakis V.J. (2010) Ion exchange and adsorption fixed bed operations for wastewater treatment - part I: modelling fundamentals and hydraulics analysis. *Journal of Engineering Studies and Research*, **16**, 29–41.

Ko D.C.K., Porter J.F. & McKay G. (1999) Optimized correlations for the fixed-bed adsorption of metal ions on bone char. *Chemical Engineering Science*, **55**, 5819–5829.

Lodeiro. P., Herrero R. & Sastre de Vicente M.E. (2006) The use of protonated Sargassum muticum as biosorbent for cadmium removal in a fixed-bed column. *Journal of Hazardous Materials*, **B137**, 244–253.

McKay G., Yee T.F., Nassar M.M. & Magdy Y. (1998) Fixed-bed adsorption of dyes on bagasse pith. *Adsorption Science & Technology*, **16**, 623–640.

Nuić I., Trgo M., Perić J. & Vukojević Medvidović N. (2013) Analysis of breakthrough curves of Pb and Zn sorption from binary solutions on natural clinoptilolite. *Microporous and Mesoporous Materials*, **167**, 55–61.

Perić J., Trgo M., Vukojević Medvidović N. & Nuić I. (2009) The effect of zeolite fixed bed depth on lead removal from aqueous solutions. *Separation Science and Technology*, **44**, 3113–3127.

Qaiser S., Saleemi A.R. & Ahmad M.M. (2007) Heavy metal uptake by agro-based waste materials. *Electronic Journal of Biotechnology*, **10**, 409–416.

Rajeshkannan R., Rajasimman M. & Rajamohan N. (2013) Packed bed column studies for the removal of dyes using novel sorbent. *Chemical Industry & Chemical Engineering Quarterly*, **19**, 461–470.

Remenárová L., Pipiška M., Hornik M., Rozložník M., Augustin J. & Lesný J. (2012) Biosorption of cadmium and zinc by activated sludge from single and binary solutions: Mechanisms, equilibrium and experimental design study. *Journal of the Taiwan Institute of Chemical Engineers*, **43**, 433–443.

Trgo M., Vukojević Medvidović N. & Perić J. (2011) Application of mathematical empirical models to dynamic removal of lead on natural zeolite clinoptilolite in a fixed bed column. *Indian Journal of Chemical Technology*, **18**, 123–131.

Vijayaraghavan K. & Praba D. (2006) Potential of Sargassum wightii biomass for copper(II) removal from aqueous solutions: Application of different mathematical models to batch and continuous biosorption data. *Journal of Hazardous Materials*, **B137**, 558–564.

Vukojević Medvidović N., Perić J. & Trgo M. (2006) Column performance in lead removal from aqueous solutions by fixed bed of natural zeolite-clinoptilolite. *Separation and Purification Technology*, **49**, 237–244.

Wan Ngah W.S., Teong L.C., Toh R.H. & Hanafiah M.A.K.M. (2012) Utilization of chitosan-zeolite composite in the removal of Cu(II) from aqueous solution: Adsorption, desorption and fixed bed column studies. *Chemical Engineering Journal*, **209**, 46–53.

https://doi.org/10.1180/claymin.2015.050.1.09 Published online by Cambridge University Press